The Bang-Bang Hysteresis Current Waveshaping Control Technique Used to Implement a High Power Factor Power Supply

Luiz Henrique Silva Colado Barreto, Ernane Antônio Alves Coelho, *Member, IEEE*, Valdeir José Farias, Luiz Carlos de Freitas, and João Batista Vieira, Jr.

***Abstract*—This work reports the operation and development of a high power factor power supply that operates at high switching frequency. An optimum power factor correction is obtained using an ac–dc boost converter associated to a nondissipative snubber as a pre-regulator circuit, which presents reduced commutation losses. The same nondissipative snubber is associated to a Forward converter and then used as a dc–dc stage. The proposed switched mode power supply presents high power factor (0.998), high efficiency (91%), low harmonic content (current and voltage total harmonic distortion rates equal to 2.84% and 2.83%, respectively), and also satisfactory regulation. The converter has been theoretically analyzed, designed, simulated and implemented, where experimental results show that soft commutation in all switches is achieved.**

***Index Terms*—AC–DC boost converter, dc–dc stage, forward converter, harmonic content, harmonic distortion, power factor correction, snubber, soft commutation.**

I. Introduction

In THE LAST few years, power factor correction, minimization of harmonic content and electromagnetic interference (EMI) levels, as well as reduction of size, weight and cost of switching mode power supplies (SMPS) has become the main concern of industry and academic researchers, as they present higher output dc voltage levels, constant switching frequency, reduced size and weight if compared to linear power supplies.

However, the input stages of switching mode power supplies are potential harmonic sources. Recently, there has been great interest about the reduction of input current harmonic content and power factor correction (PFC). Moreover, in many single-phase applications, mainly in power supplies, the power levels can reach several kilowatts and, in some cases, the input voltage can be quite high as well. For such types of application, the conventional Boost PFC converter has been intensively used due to its intrinsic characteristics of dc-voltage gain, lower inductor volume and weight, and losses on the power devices, which will affect converter cost, efficiency, and power density [1] and [2]. An adequate modulation technique is necessary so that high power factor and low harmonic distortion can be achieved, as this work employs the Bang-Bang hysteresis current waveshaping control technique [9], [11], [12] for this purpose.

Moreover, the Boost converter presents commutation and conduction losses, implying the reduction of efficiency. Conventional resonant and quasiresonant converters [3] and [4] provide zero-current switching (ZCS) and/or zero-voltage switching (ZVS) [5] and [6]. Such converters can operate at high frequencies, although they present load limitation, because there are current and/or voltage peaks over the switches and a specific range to control the frequency, as the design of filters becomes complex. A satisfactory alternative to achieve high frequency and high-power operation lies in the use of nondissipative snubbers [7].

DC/DC converters provide the conversion of distinct voltage levels in switching mode power supply. Several dc–dc converters can be used, but it is necessary that they operate at high frequency and also present reduced switching losses, multiple regulated outputs and isolation. The proposed SMPS employs a dc–dc Forward converter using a nondissipative snubber to achieve such optimum performance, as it is suitable to the required power level and provides soft switching a wide load range, as the conduction losses are almost the same as those observed in the hard-switched PWM converter.

This paper presents a switching mode power supply composed by a PFC Boost converter and a Forward converter, as both them use a resonant cell to reduce commutation losses, according to Fig. 1. The proposed SMPS employs the Bang-Bang hysteresis current waveshaping control technique to achieve high power factor and low harmonics distortion.

II. Proposed SMPS

The ac–dc and dc–dc nondissipative converters are shown in Figs. 2 and 3, which operate with reduced commutation losses. In the proposed SMPS, main switches S_1 (Boost) and S_1' (Forward) are commutated in a ZVS way, and auxiliary switches S_2 (Boost) and S_2' (Forward) are commutated in a ZCS way due to the resonant cell, composed of resonant inductors (L_r and L_r') and resonant capacitors (C_{r1}, C_{r2}, C_{r1}', and C_{r2}'). High power factor is obtained using the Bang-Bang Hysteresis current waveshaping control technique.

In order to simplify the analysis, the converters are analyzed apart.

Manuscripts received December 13, 2002; revised May 13, 2003. This work was supported by Thorton Inpec, Siemens, Texas Instruments, CAPES, CNPQ, and FAPEMIG. Recommended by Associate Editor C. K. Tse.

E. A. A. Coelho, V. J. Farias, L. C. de Freitas, and J. B. Vieira, Jr. are with the Faculdade de Engenharia Elétrica, Universidade Federal de Uberlândia, Campus Santa Mônica—Bloco "3N," Uberlândia 38400-902, Brazil (e-mail: batista@ufu.br).

L. H. S. C. Barreto is with the Electrical Engineering Department, Federal University of Ceará, Ceará, Brazil (e-mail: luizhbarreto@yahoo.com.br).

Digital Object Identifier 10.1109/TPEL.2003.820591

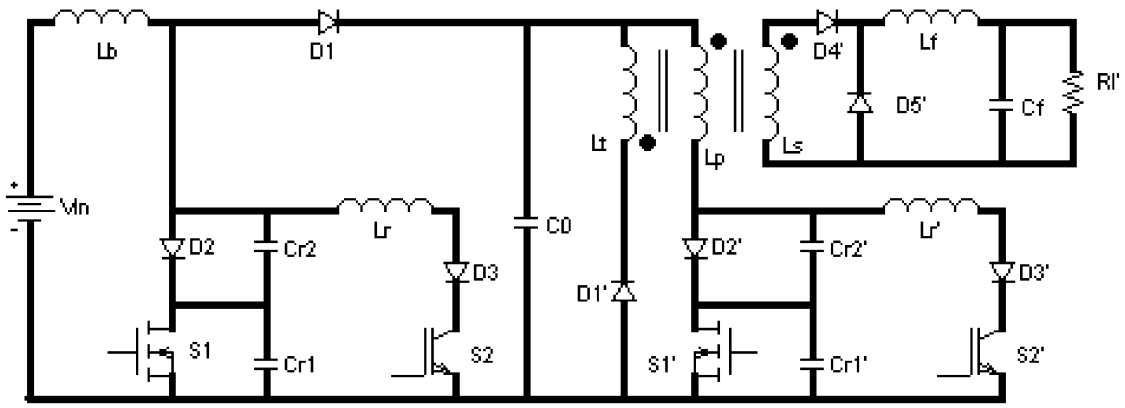

Fig. 1. Proposed switching mode power supply.

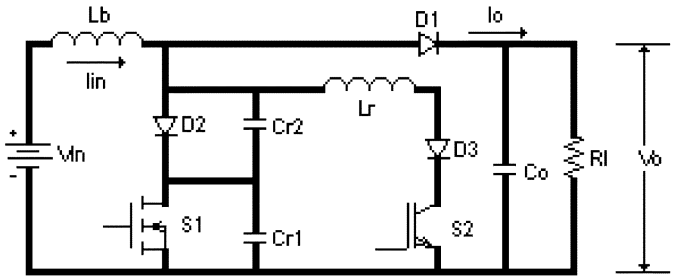

Fig. 2. Boost converter associated to a nondissipative snubber.

III. Principle of Operation of the AC–DC Boost Converter

A complete theoretical analysis for the approach shown in Fig. 2 is presented as follows. Since both converters present the same principle of operation, a single Boost converter will be analyzed.

The analysis begins with the description of seven operationg stages that determine a complete switching cycle.

1) First stage (t_0-t_1) Fig. 4—This stage begins when switch S_2 is turned on in a ZCS way, where resonant current I_{Lr} increases linearly. It finishes when I_{Lr} is equal to input current I_{in}.
2) Second Stage (t_1-t_2) Fig. 5—When the resonant current is equal to the input current, this stage begins. This is the first resonant stage, where both resonant capacitors (C_{r1} and C_{r2}) are in resonance with inductor L_r, during which capacitor C_{r1} is discharged and capacitor C_{r2} is charged to its reverse condition. It finishes when C_{r1} is fully discharged, allowing switch S_1 to be turned on in a ZVS way.
3) Third stage (t_2-t_3) Fig. 6—This is the second resonant stage, during which capacitor C_{r2} is in resonance with inductor L_r. Moreover, switch S_1 is turned on in a ZVS way. It finishes when resonant current I_{Lr} reaches null.
4) Fourth stage (t_3-t_4) Fig. 7— This stage begins when current I_{Lr} is null. Resonant capacitor C_{r2} is linearly fully discharged by input current I_{in}. Moreover, switch S_2 can be turned off in a ZCS way.
5) Fifth stage (t_4-t_5) Fig. 8—When capacitor C_{r2} is fully discharged, this stage begins, where the input source transfers its energy to boost inductor L_b. It finishes when switch S_1 is turned off in ZVS way.
6) Sixth stage (t_5-t_6) Fig. 9—When switch S_1 is turned off, capacitor C_{r1} is linearly charged by input current I_{in} up to output voltage V_0, which represents the end of this stage.
7) Seventh stage (t_6-t_7) Fig. 10—During this stage, the stored energy in the Boost inductor L_b is transferred to the load. It finishes as a new switching cycle begins.

The transference function between V_0 and V_{in} is given by

$$G=\frac{V_0}{V_{in}}=\frac{1}{1-\left\{D+\frac{K_1}{2\pi}\left[\arccos\left(-\frac{1}{X}\right)+\frac{X+1}{X\alpha}+\frac{\alpha}{2}\right]\right\}} \quad (1)$$

where

f_s switching frequency;
f_0 resonant frequency;
D duty cycle;
X ratio between C_{rl} and C_{r2};

$$\alpha=\frac{I_{in}}{V_0}\sqrt{\frac{L_r}{C_r}} \quad (2)$$

$$K_1=\frac{f_s}{f_0}. \quad (3)$$

From the operating stages described above, one can obtain the waveforms shown in Fig. 11.

IV. Principle of Operation of the DC–DC Forward Converter

Fig. 3 shows the Forward converter associated to a nondissipative snubber employed as a dc–dc stage.

From the operating stages, which are basically the same as those of the Boost converter, one can obtain the waveforms shown in Fig. 12.

The transfer function between V_o' and V_{in}' is given by

$$G'=\frac{V_0'}{V_{in}'}=\frac{n_s}{n_p}\left\{D'+\frac{K_1'}{2\pi}\left[\arccos\left(\frac{-1}{X'}\right)+\frac{X'+1}{X'\alpha'}+\frac{\alpha'}{2}\right]\right\} \quad (4)$$

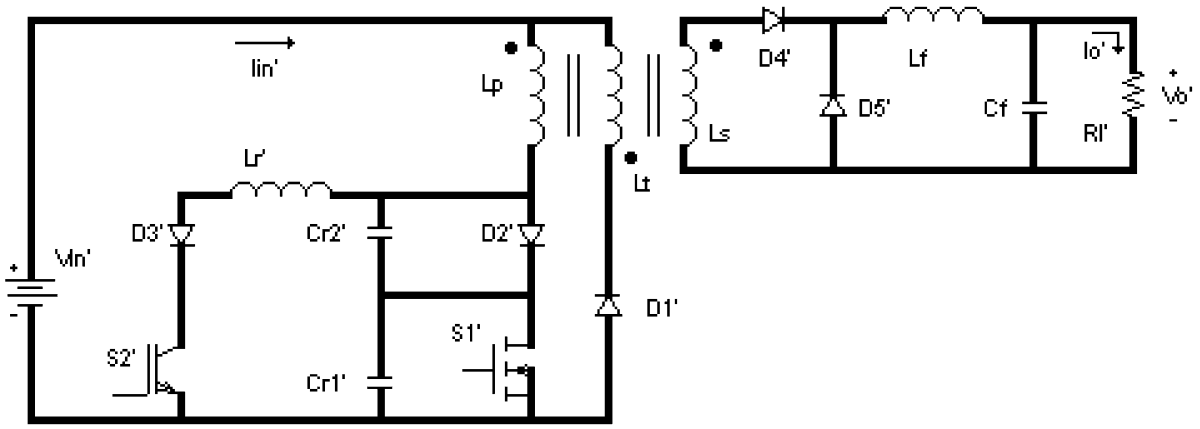

Fig. 3. Forward converter associated to a nondissipative snubber.

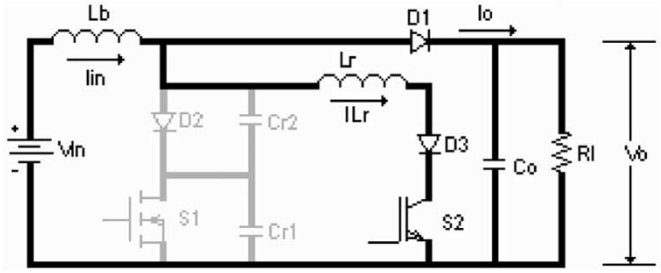

Fig. 4. First stage.

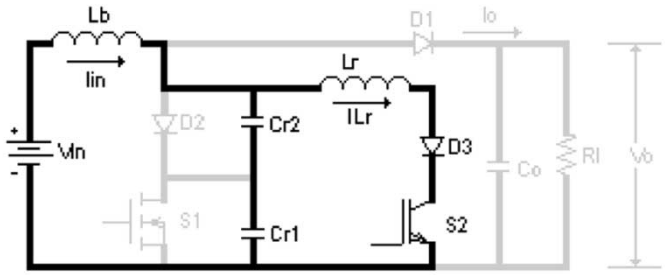

Fig. 5. Second stage.

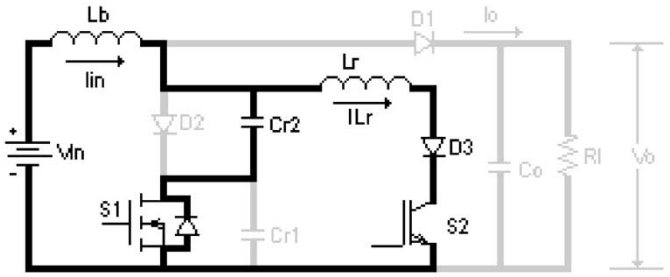

Fig. 6. Third stage.

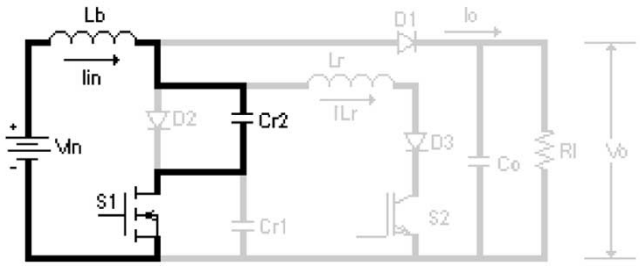

Fig. 7. Fourth stage.

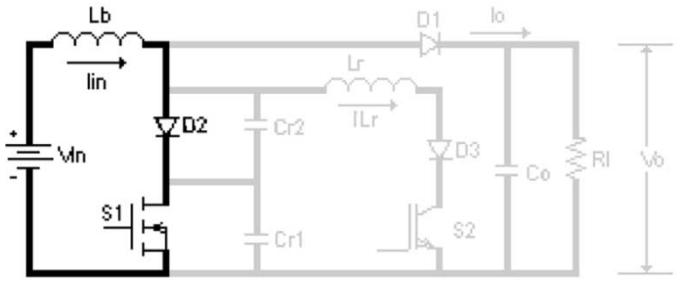

Fig. 8. Fifth stage.

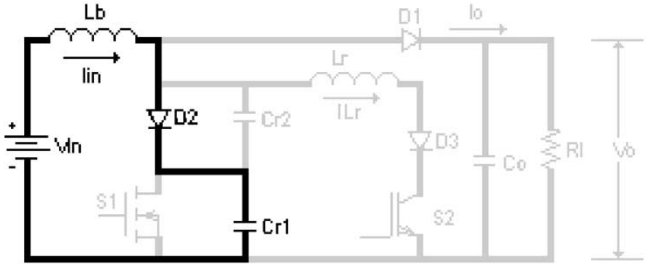

Fig. 9. Sixth stage.

where

n_p number of primary turns;
n_s number of secondary turns;
f_s' Switching frequency;
f_o' resonant frequency;
D' duty cycle;
X' ratio between C_{rl}' and C_{r2}';

$$\alpha' = \frac{I_{in}'}{V_{in}'}\sqrt{\frac{L_r'}{C_r'}} \tag{5}$$

$$K_1' = \frac{f_s'}{f_0'}. \tag{6}$$

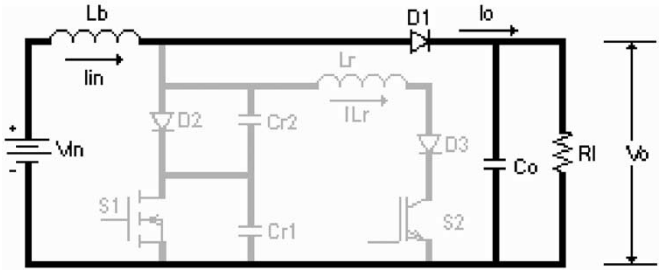

Fig. 10. Seventh stage.

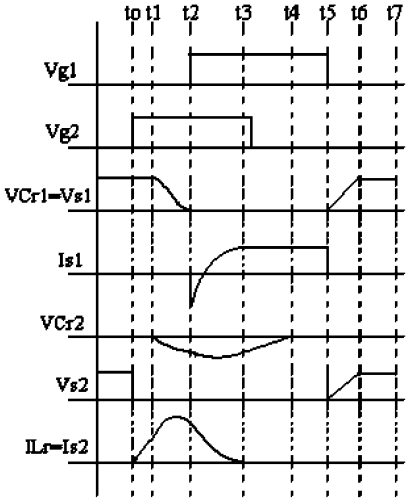

Fig. 11. Theoretical waveforms for Boost converter associated to a nondissipative snubber.

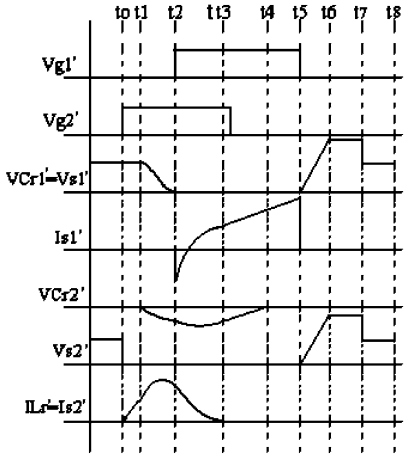

Fig. 12. Theoretical waveforms for the forward converter associated to a nondissipative snubber.

V. Plane Graph

Fig. 13 shows the phase plane graph of the proposed Boost converter and Fig. 14 shows the phase plane graph of the proposed Forward converter. Once that the converters present two resonant frequencies, the phase plane graph must be separated in schemes.

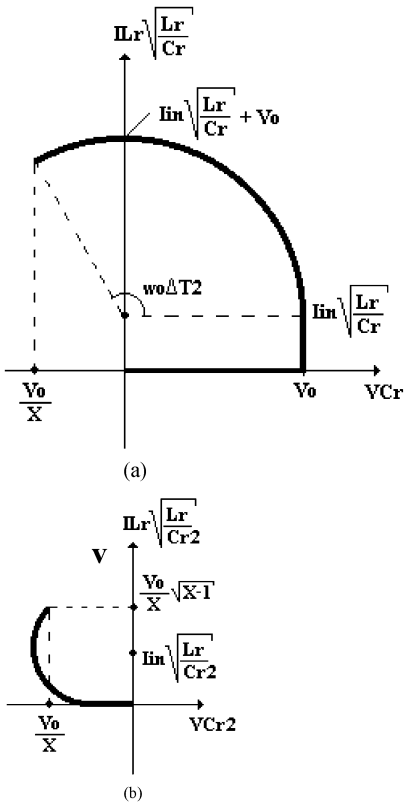

Fig. 13. Phase plane graph of the boost converter.

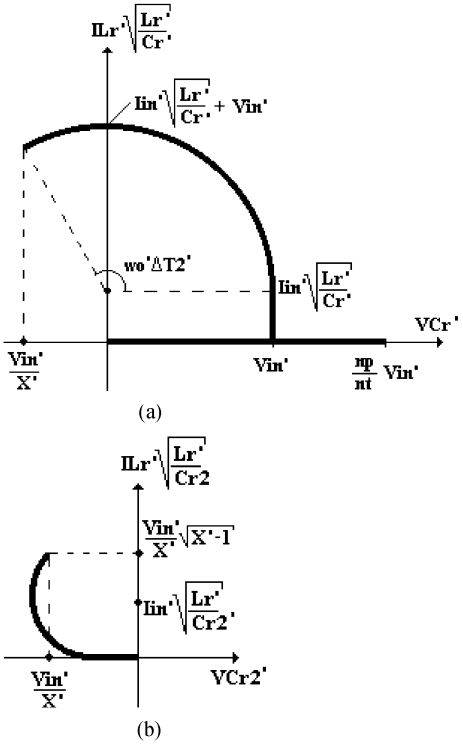

Fig. 14. Phase plane graph of the forward converter.

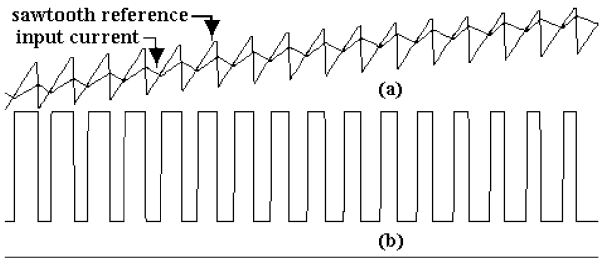

Fig. 15. Bang-bang hysteresis current waveshaping technique with fixed switching frequency: (a) input current waveform and (b) boost switch gating signal.

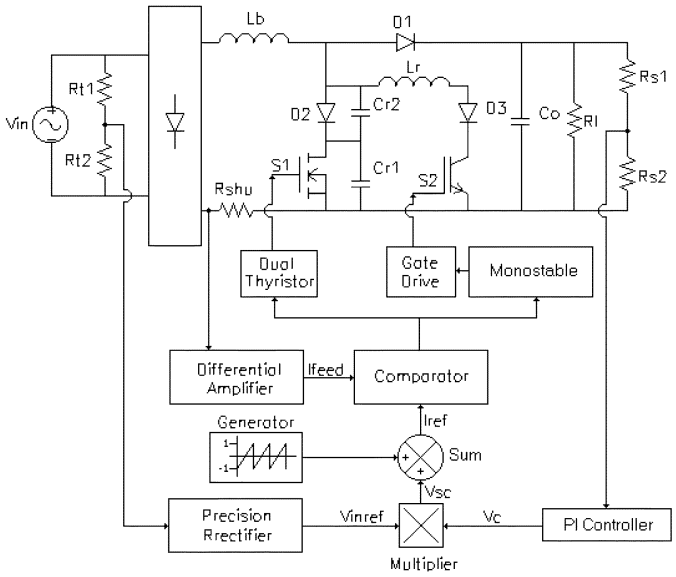

Fig. 16. Boost converter associated to the nondissipative snubber and the control circuit.

The analysis of the phase plane graphs shown above provides the soft commutation range limits. The Boost converter presents soft commutation only if the following condition is valid:

$$1 \leq X \leq \frac{1}{4\alpha_2^2} + 1. \tag{7}$$

Moreover, the Forward converter presents soft commutation only if

$$1 \leq X' \leq \frac{1}{4\alpha_2'^2} + 1. \tag{8}$$

VI. Control Strategy

Fig. 15 shows the control strategy adopted in this paper [9], [11].

The block diagram of the control circuit with the Boost power stage is shown in Fig. 16. This converter operates with constant switching frequency and high power factor, using the Bang-Bang current control strategy.

The input current and line voltage samples are obtained from sensors R_{shu} and R_{t1}/R_{t2}, respectively. The voltage sample is rectified in the Precision Rectifier block.

The PI controller is implemented to provide the signal control (Vc), which is multiplied by the voltage reference signal (V_{inref}). This signal is then added to the sawtooth signal generating the reference current signal (I_{ref}). Drive signals are achieved comparing the current feedback signal, obtained in the R_{shu} sensor, with the reference current signal.

The signal obtained from the output comparator block is driven directly to monostable, to provide a fixed pulse, and driven to auxiliary switch S_2. The same signal will drive switch S_1, when the zero voltage transition on the switch is satisfied, which is possible because switch S_1 is driven in a dual thyristor mode.

VII. Simulation and Experimental Results

The switched mode power supply proposed in this paper (Fig. 1) has been intensively studied via simulation using PSpice software, where the following parameter set is employed:

S_1 and $S_1' = IrfP460$;
S_2 and $S_2' =$ Ideal;
$L_f = 100\ \mu$H;
$C_f = 1$ mF;
D_3 and $D_3' =$ Ideal;
remaining diodes = MUR1560;
$V_{in} = \sim 110$ V;
$V_0 = 200$ V;
$C_{r1} = 10$ nf;
$C_{r1}' = 7.5$ nf;
$V_0' = 50$ V;
$I_0' = 12$ A;
$C_{r2} = 27$ nf;
$C_{r2}' = 47$ nf;
$f_S = 100$ kHz;
$C_0 = 680\ \mu$F;
L_r and $L_r' = 2.5\ \mu$H;
$L_b = 1.5$ mH;
$P_0 = 600$ W.

A prototype of the proposed switched mode power supply has been built using the following parameter set.

S_1 and $S_1' = IrfP460$.
S_2 and $S_2' =$ IRGBC20 f.
$L_f = 100\ \mu$H;
$C_f = 1$ mF;
$D_1' = 2\times$ MUR1560;
remaining diodes = MUR1560;
$V_{in} = \sim 110$ V;
$V_0 = 200$V;
$C_{r1} = 10$ nf;
$C_{r1}' = 7.5$ nf;
$V_0' = 50$ V;
$I_0' = 12$ A;
$C_{r2} = 27$ nf;
$C_{r2}' = 47$ nf;
$f_S = 100$ kHz;
$C_0 = 680\ \mu$F;
L_r and $L_r' = 2.5\ \mu$H;
$L_b = 1.5$ mH;
$P_0 = 600$ W.

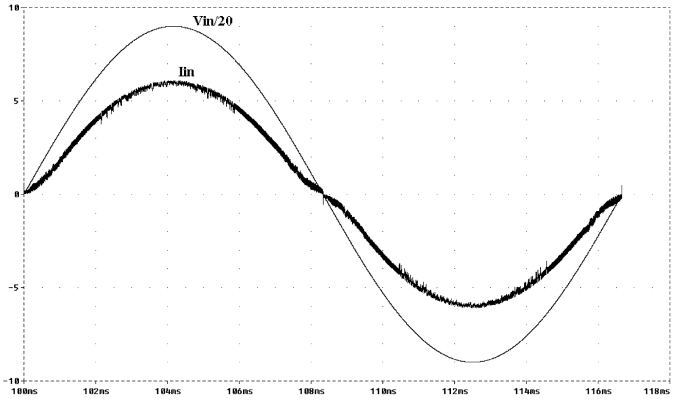

(a)

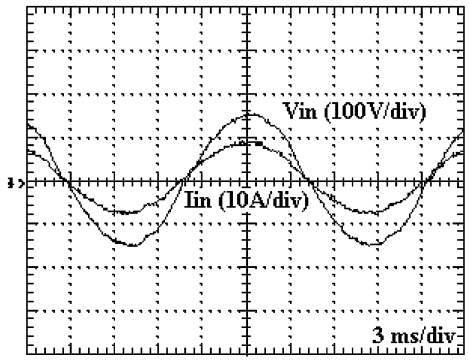

(b)

Fig. 17. Input voltage and input current for nominal load: (a) simulated results and (b) experimental results.

The Boost inductor (L_b) was built using core EE 65/33/26 with 17 turns and 4×18 AWG, and the resonant inductors (L_r and L_r') are coreless, with diameter 2.54 cm (1') and nine turns using wire 12 AWG.

Figs. 17–21 show the simulation and experimental results. As it can be seen, the commutations occur with reduced losses and the power factor is almost unity. Fig. 17 shows the power factor correction, as the value obtained in the nominal load is 0.998.

Current and voltage total harmonic distortion rates are shown in Fig. 18, where the current THD was obtained in simulation and experimentally, and the voltage THD was obtained only in the prototype. In the simulation, the current THD value is equal to 4.85%, and in the prototype the current and voltage THD values are 2.84% and 2.83%, respectively. A comparison between experimental values obtained in the proposed switched mode power supply and IEC 61 000–3-2 standard [10] is presented in Table I, where it can be seen that the values of the harmonic individual components are below the standard limits.

Current and voltage total harmonic distortion rates are shown in Fig. 18, where the current THD was obtained in simulation and experimentally, and the voltage THD was obtained only in the prototype. In the simulation, the current THD value is equal to 4.85%, and in the prototype the current and voltage THD values are 2.84% and 2.83%, respectively. A comparison between experimental values obtained in the proposed switched mode power supply and IEC 61 000–3-2 standard [10] is

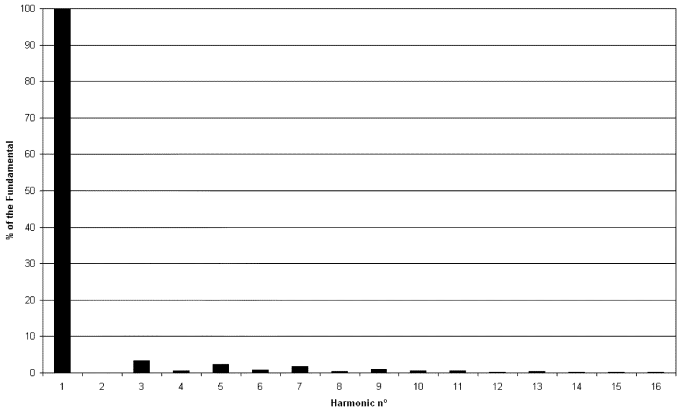

(a)

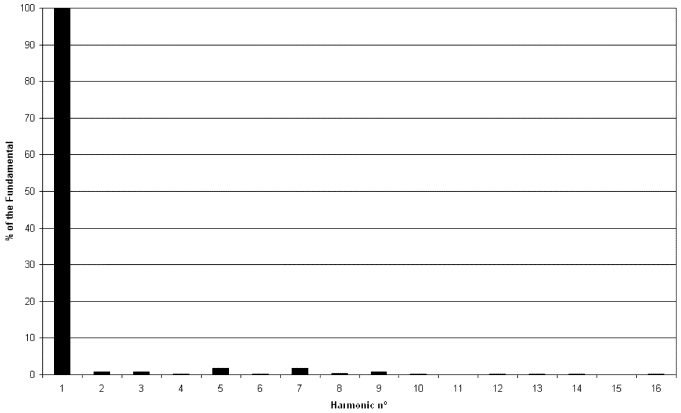

(b)

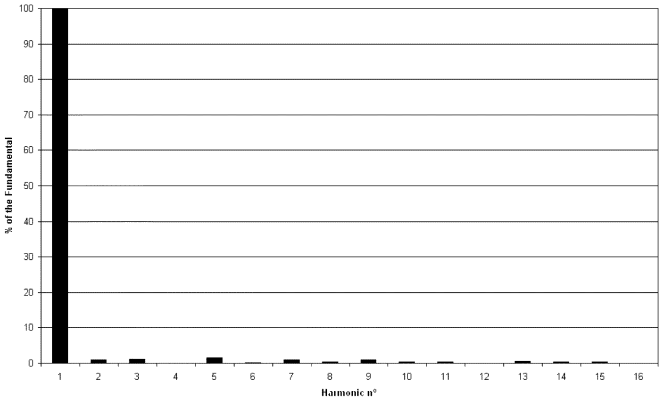

(c)

Fig. 18. Harmonic content: (a) input current concerning simulated results, (b) input voltage concerning experimental results, and (c) input current concerning experimental results.

presented in Table I, where it can be seen that the values of the harmonic individual components are below the standard limits.

Figs. 19 and 20 show the commutation in the active switches. It can be seen that the main switches do not present current and/or voltage stresses, as well as the commutations are nondissipative, and the auxiliary switches commutate in a ZCS way.

Fig. 21 shows the efficiency graph of the proposed switched mode power supply. An average efficiency equal to 90.6% has been achieved.

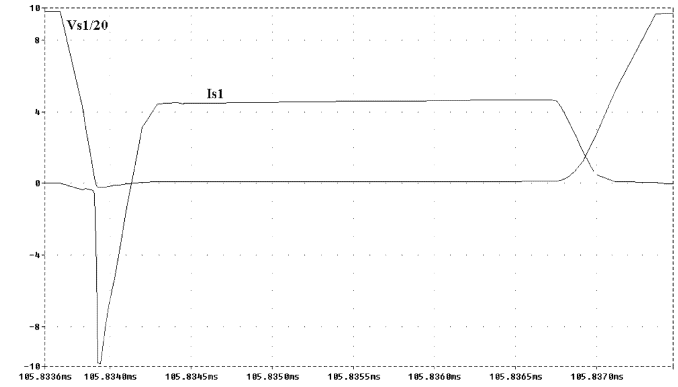

(a)

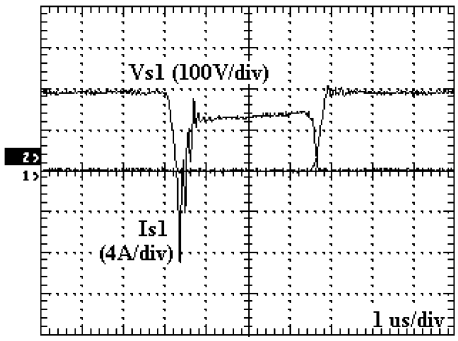

(b)

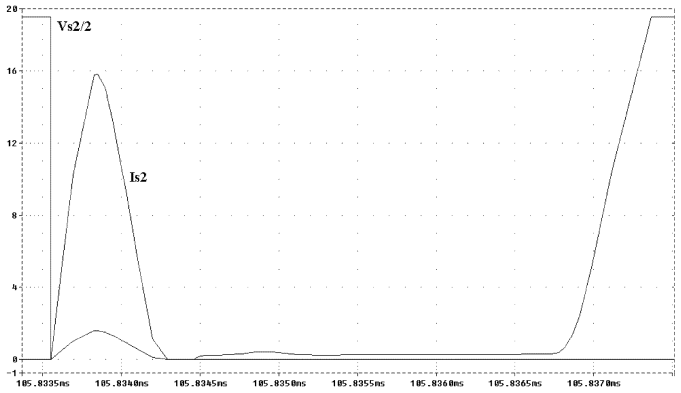

(c)

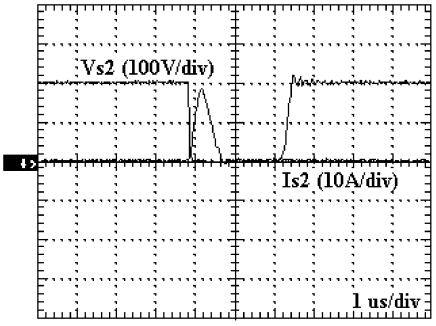

(d)

Fig. 19. Active switches in boost converter: (a) Main switch S1 waveforms concerning simulated results, (b) main switch S1 waveforms concerning experimental results, (c) auxiliary switch S2 waveforms concerning simulated results, and (d) auxiliary switch S2 waveforms concerning experimental results.

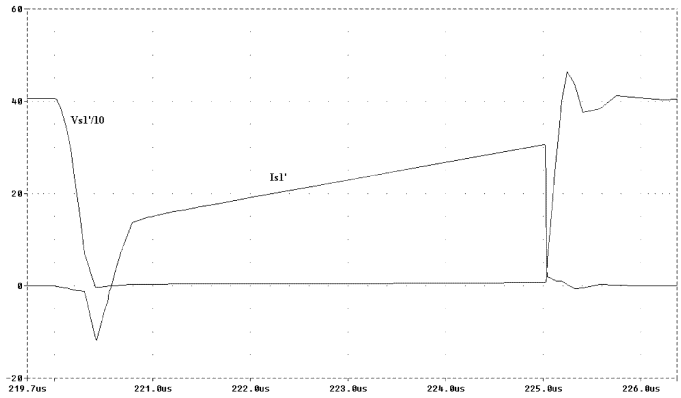

(a)

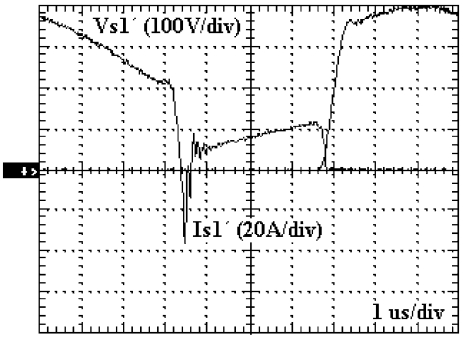

(b)

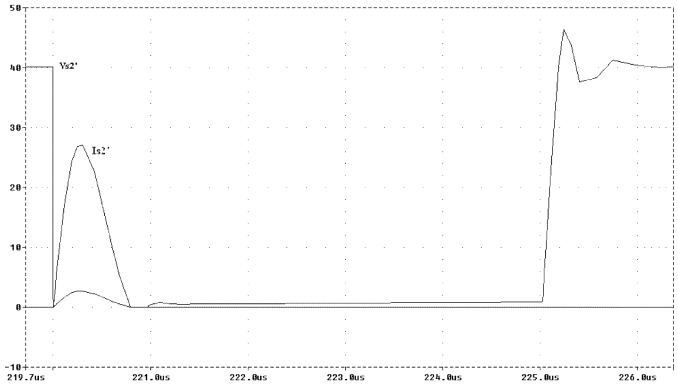

(c)

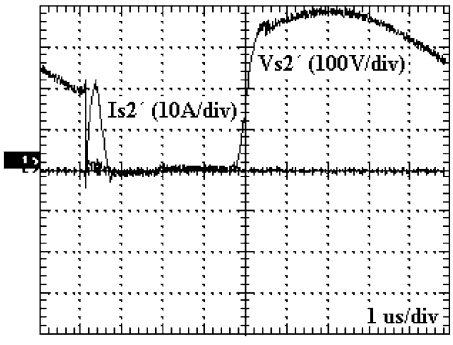

(d)

Fig. 20. Active switches of the forward converter: (a) main switch S_1' waveforms concerning simulated results, (b) main switch S_1' waveforms concerning experimental results, (c) auxiliary switch S_2' waveforms concerning simulated results, and (d) auxiliary switch S_2' waveforms concerning experimental results.

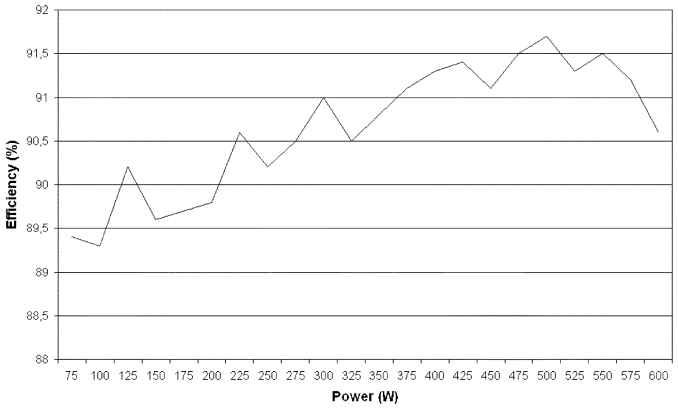

Fig. 21. Efficiency.

TABLE I
HARMONIC CONTENT OF THE INPUT CURRENT COMPARED TO THE LIMITS IMPOSED BY IEC 61 000-3-2 STANDARD

Harmonic Order	Experimental values	IEC 61000-3-2 standard
	Nominal current 5.79A	Nominal current 16A
Odd	%	%
3	1.28	14.4
5	1.63	7.1
7	1.04	4.8
9	0.99	2.5
11	0.40	2.1
13	0.53	1.3
15	0.34	0.94
Even		
2	0.97	6.8
4	0.08	2.7
6	0.16	1.9
8	0.33	1.4
10	0.35	1.15
12	0.07	0.95
14	0.38	0.82
16	0.07	0.72

VIII. CONCLUSION

This paper reports the analytical, simulation and experimental developments of a SMPS using the PFC ac–dc Boost associated to a nondissipative snubber. It has been demonstrated that the use of the Bang-Bang Hysteresis current waveshaping control technique in combination with the nondissipative snubber implies a highly efficient power factor correction pre-regulator circuit with reduced commutation losses.

The proposed SMPS employs a Forward converter as a dc–dc converter, which operates with soft commutation by using a nondissipative snubber. The harmonic reduction and power factor correction is much improved if compared to results presented in recent literature [13]–[15].

The objective initially proposed was achieved, where a switching mode power supply with power factor correction (0.998), high efficiency (90.6%), low harmonic distortion rates (current and voltage THD values equal to 2.84% and 2.83%, respectively) and satisfactory regulation was theoretically analyzed, projected, simulated, and implemented.

REFERENCES

[1] M. T. Zhang, Y. Jiang, F. Lee, C. Joavanovic, and M. Milam, "Single-phase three-level boost power factor correction converter," in *Proc. IEEE APEC*, 1995, pp. 434–439.
[2] B. A. Miwa, D. M. Otten, and M. F. Schlecht, "High efficiency power factor corretion using interleaving techniques," in *Proc. IEEE APEC*, 1992, pp. 368–375.
[3] F. C. Lee, "High-Frequency quasiresonant converter technologies," *Proc. IEEE*, vol. 76, pp. 377–390, Apr. 1988.
[4] I. Barbi, J. C. Bolacell, and J. B. Vieira, Jr, "A forward pulse-width modulated quasiresonant converter: Analysis, design and experimental results," in *Proc. IEEE IECON*, 1989, pp. 21–26.
[5] F. C. Lee, G. Hua, and C. S. Leu, "Novel zero-voltage-transition PWM converters," in *Proc. IEEE PESC*, 1992, pp. 55–61.
[6] V. J. de Freitas, P. S. Farias, J. B. Vieira Jr, H. L. Hey, and D. F. Cruz, "An optimum ZVS-PWM dc-to-dc converter family: Analysis, simulation and experimental results," in *Proc. IEEE PESC*, 1992, pp. 229–235.
[7] L. H. S. C. Barreto, A. A. Pereira, V. J. Farias, L. C. de Freitas, and J. B. Vieria Jr, "A boost converter associated with a new nondissipative snubber," in *Proc. IEEE APEC*, 1998, pp. 1077–1083.
[8] L. H. S. C. Barreto, A. A. Pereira, V. J. Farias, L. C. de Freitas, and J. B. de Vieira Jr, "A nondissipative snubber applied to the FORWARD-PWM-ZVS-SR," in *Proc. CIEP*, 2000.
[9] R. Tóffano Jr, C. H. G. Treviso, V. J. Farias, J. B. Vieira Jr, and L. C. de Freitas, "A self-resonant-PWM boost converter with unity power factor operation by using bang-bang current control strategy with fixed switching frequency," in *Proc. EPE*, 1997, pp. 4.454–4.457.
[10] "Electromagnetic compatibility (EMC)—Part 3—2—Limits for harmonic current emissions (equipment input current $\leq$16 A per phase)," Tech. Rep., IEC 61 000-3-2.
[11] M. Kazerani, G. Joos, and P. D. Ziogas, "A novel active current waveshaping technique for solid state input power factor conditioners," in *Proc. IEEE IECON*, 1989, pp. 99–105.
[12] K. Fung, W. Ki, and K. T. M. Philip, "Analysis and measurement of DCM power factor correctors," in *Proc. IEEE PESC*, 1999.
[13] T. F. Wu, Y. J. Wu, and Y. C. Liu, "Development of converters for improving efficiency and achieving both power factor correction and fast output regulation," in *Proc. IEEE APEC*, 1999.
[14] C. A. Gallo, J. A. C. Pinto, L. C. de Freitas, V. J. Farias, E. A. A. Coelho, and J. B. Vieira Jr, "An unity high power factor power supply rectifier using a PWM ac/dc full bridge soft—switching," in *Proc. IEEE APEC*, 2002.
[15] D. Li, X. Ruan, H. Xu, and Y. Yan, "A hybrid single-switch power factor correction pre-regulator," in *Proc. IEEE PESC*, 2002.

Luiz Henrique Silva Colado Barreto was born in Naviraí, Brazil, on June 15, 1974. He received the B.S. degree in electrical engineering from the Federal University of Mato Grosso, Brazil, in 1997 and the M.S. and Ph.D. degrees from the Federal University of Uberlândia, Brazil, in 1999 and 2003, respectively.

He is a Visiting Professor of the Electrical Engineering Department, Federal University of Ceará, Brazil. His research interest areas include high-frequency power conversion, modeling and control of converters, power factor correction circuits, new converters topologies, UPS system, and fuel cell.

Ernane Antônio Alves Coelho (M'02) was born in Teófilo Otoni, Brazil, on April 1, 1962. He received the B.S. degree in electrical engineering from the Federal University of Minas Gerais, Brazil, in 1987, the M.S. degree from the Federal University of Santa Catarina, Florianópolis, Brazil, in 1989, and the M.S. and Ph.D. degrees from the Federal University of Minas Gerais, in 2000.

He is a Titular Professor of the Electrical Engineering Faculty, Federal University of Uberlândia, Brazil. His research interests include PWM inverters, factor correction circuits and new converters topologies, and digital control using DSPs.

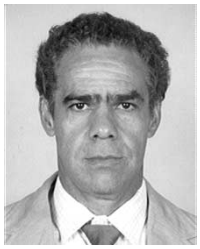

Valdeir José Farias was born in Araguari, Brazil, on November 18, 1947. He received the B.S. degree in electrical engineering from the Federal University of Uberlândia (UFU), Brazil, in 1975, the M.S. degree in power electronics from the Federal University of Minas Gerais (UFMG), Brazil, in 1981, and the Ph.D. degree State University of Campinas (UNICAMP), Brazil, in 1989.

He is a Titular Professor of the Electrical Engineering Faculty, Federal University of Uberlândia, Brazil. His research interests are power electronics in general, specially soft-switching converters and active power filters.

Dr. Farias is a member of SBA and the Brazilian Society of Power Electronics (SOBRAEP).

Luiz Carlos de Freitas was born in Monte Alegre de Minas, Brazil, on April 1, 1952. He received the B.S. degree in electrical engineering from the Federal University of Uberlândia, Brazil, in 1975 and the M.S. and Ph.D. degrees from the Federal University of Santa Catarina, Brazil, in 1985 and 1992, respectively.

He is a Titular Professor of the Electrical Engineering Faculty, Federal University of Uberlândia, Brazil. He has two Brazilian patents pending. His research interest areas include high-frequency power conversion, modeling and control of converters, power factor correction circuits, and new converters topologies.

Dr. de Freitas is a member of SBA and the Brazilian Society of Power Electronics (SOBRAEP).

João Batista Vieira, Jr. was born in Panamá-Go, Brazil, on March 23, 1955. He received the B.S. degree in electrical engineering from the Federal University of Uberlândia, Brazil, in 1980 and the M.S. and Ph.D. degrees from the Federal University of Santa Catarina, Brazil, in 1984 and 1991, respectively.

He began work as an Instructor with the Electrical Engineering Department, Federal University of Uberlândia (UFU), in 1980. He is a Titular Professor of the Electrical Engineering Faculty, Federal University of Uberlândia. His research interest areas include high-frequency power conversion, modeling and control of converters, power factor correction circuits, and new converters topologies.

Dr. Vieira is a member of SBA and the Brazilian Society of Power Electronics (SOBRAEP).